

Predictions of Energy Savings in HVAC Systems by Lumped Models

A.P. Wemhoff^{a,*}, M.V. Frank^b

^a*Dept. of Mechanical Engineering, Villanova University, Villanova, PA 19085*

^b*Code 985, Naval System Warfare Center, Carderock Division, Philadelphia, PA 19112*

Abstract

An approach to optimizing the energy efficiency of a Heating, Ventilating, and Air Conditioning (HVAC) system is presented that utilizes computational predictions of the effect of heat load distribution on moist air temperature, density, and humidity variation. Lumped-HVAC (L-HVAC) is a new lumped parameter code that couples fluid transport, energy transport, thermodynamics, and psychrometrics in an HVAC system. This code contains a nonlinear implicit solution algorithm for steady-state and transient calculations for flow resistance, water mass balance, and energy conservation. L-HVAC has been validated using a simplified analytical model, the commercial lumped parameter code SINDA/FLUINT, and experimental measurements. Steady-state calculations for a single-room system suggest an order of magnitude greater energy savings using a variable chiller power control approach compared to control damper and variable-drive fan approaches. L-HVAC was also applied to predict that the fraction of latent to total heat load influences the steady-state system temperature by up to 0.4°C for the example system in this study.

Keywords: lumped analysis, energy management, HVAC system, psychrometrics

1. Introduction

Heating, Ventilating, and Air Conditioning (HVAC) systems comprise a large portion of energy use in today's buildings. In 2001, the Department of

*Corresponding author

Report Documentation Page				Form Approved OMB No. 0704-0188	
Public reporting burden for the collection of information is estimated to average 1 hour per response, including the time for reviewing instructions, searching existing data sources, gathering and maintaining the data needed, and completing and reviewing the collection of information. Send comments regarding this burden estimate or any other aspect of this collection of information, including suggestions for reducing this burden, to Washington Headquarters Services, Directorate for Information Operations and Reports, 1215 Jefferson Davis Highway, Suite 1204, Arlington VA 22202-4302. Respondents should be aware that notwithstanding any other provision of law, no person shall be subject to a penalty for failing to comply with a collection of information if it does not display a currently valid OMB control number.					
1. REPORT DATE 14 APR 2010		2. REPORT TYPE		3. DATES COVERED 00-00-2010 to 00-00-2010	
4. TITLE AND SUBTITLE Predictions of Energy Savings in HVAC Systems by Lumped Models				5a. CONTRACT NUMBER	
				5b. GRANT NUMBER	
				5c. PROGRAM ELEMENT NUMBER	
6. AUTHOR(S)				5d. PROJECT NUMBER	
				5e. TASK NUMBER	
				5f. WORK UNIT NUMBER	
7. PERFORMING ORGANIZATION NAME(S) AND ADDRESS(ES) Dept. of Mechanical Engineering, Villanova University, Villanova, PA, 19085				8. PERFORMING ORGANIZATION REPORT NUMBER	
9. SPONSORING/MONITORING AGENCY NAME(S) AND ADDRESS(ES)				10. SPONSOR/MONITOR'S ACRONYM(S)	
				11. SPONSOR/MONITOR'S REPORT NUMBER(S)	
12. DISTRIBUTION/AVAILABILITY STATEMENT Approved for public release; distribution unlimited					
13. SUPPLEMENTARY NOTES					
14. ABSTRACT An approach to optimizing the energy efficiency of a Heating, Ventilating and Air Conditioning (HVAC) system is presented that utilizes computational predictions of the effect of heat load distribution on moist air temperature density, and humidity variation. Lumped-HVAC (L-HVAC) is a new lumped parameter code that couples fluid transport, energy transport, thermodynamics and psychrometrics in an HVAC system. This code contains a nonlinear implicit solution algorithm for steady-state and transient calculations for flow resistance, water mass balance, and energy conservation. LHVAC has been validated using a simplified analytical model, the commercial lumped parameter code SINDA/FLUINT, and experimental measurements. Steady-state calculations for a single-room system suggest an order of magnitude greater energy savings using a variable chiller power control approach compared to control damper and variable-drive fan approaches. L-HVAC was also applied to predict that the fraction of latent to total heat load in influences the steady-state system temperature by up to 0.4 degreeC for the example system in this study.					
15. SUBJECT TERMS					
16. SECURITY CLASSIFICATION OF:			17. LIMITATION OF ABSTRACT Same as Report (SAR)	18. NUMBER OF PAGES 20	19a. NAME OF RESPONSIBLE PERSON
a. REPORT unclassified	b. ABSTRACT unclassified	c. THIS PAGE unclassified			

Energy [1] stated that 31.2% of energy use by U. S. residential buildings is by HVAC equipment, which equates to 355.7 billion kWh. In some specialized cases, HVAC energy use is more significant: cooling energy in data centers now surpasses the computing energy! [2, 3]

The traditional HVAC design approach involves static adjustment of outlet dampers to match required airflows for assumed static loads. This approach provides a reasonable approximation of required airflows for cases of fixed loads, but in many instances the loads fluctuate greatly with time. Fluctuating transient loads are apparent in classrooms, training centers, kitchens, and eating areas. These transient loads result in periods of overcooling due to small loads followed by insufficient cooling due to large loads. In addition, multiple solutions exist for providing the adequate amount of airflow into the zones, but these result in different amounts of energy consumption.

Various approaches have been proposed or implemented in today's buildings to help save energy use in transient loading. The typical office building HVAC system applies a Variable-Air-Volume (VAV) approach to reduce cooling airflow into a room via thermostat control feedback [4]. This approach solves the problems associated with static damper placement and is inexpensive, so it is commonly implemented in newer office buildings.

The insufficiency of VAV systems lies in their limited implementation to a single building zone. The HVAC system is actually a complex arrangement of fluid systems where VAV adjustment for a single zone affects the airflow into other zones. This interdependence between each of the control devices in a typical HVAC system results in a complex control scheme that is difficult to optimize for minimal energy usage. As a result, several studies have employed optimization techniques to HVAC system models such as genetic algorithms [5] and fuzzy interference [6, 7].

This study provides an alternative approach for energy minimization in an HVAC system that is straightforward to implement in most HVAC systems. The general methodology to this approach is as follows:

- An infinite number of HVAC designs provide adequate cooling to all zones in a system with fixed heat loads. The amount of energy used by the system depends on the chosen design.
- Steady-state simulations of an HVAC system allow for predictions of HVAC system energy usage for a large number of unique designs.
- An optimization routine pinpoints the design that provides adequate

cooling yet minimizes energy usage for a system with known fixed heat loads.

- Knowledge of the instantaneous loading state in a transient system allows for estimation of the control configuration that minimizes energy for that state using multidimensional interpolation.

This paper focuses on the first two bullet points above in describing a simple predictive code that calculates the energy use and outcome of an HVAC design for a user-specified system under steady loading. Subsequent studies will apply an optimization routine to predict the HVAC design featuring minimal energy use, and then translate the optimal steady-state control configurations to transient systems. Note that this study aims to minimize energy, while other studies use electricity cost; this extension is straightforward provided electricity rates are available. Figures 1 and 2 show that the optimization routine first creates a response surface by selective sampling of control parameters, and then it optimizes the the control parameters using the response surface and a known optimization method. This approach, described in many texts (e.g. [8]) and applied in numerous studies outside of the HVAC field (e.g. [9, 10]), is similar to that by Fong et al. [11, 12], where their study optimized the parameters involved in a specific HVAC application; and Snyder and Newell [13], who calculated the effects of building mass in a lumped fashion. This study provides a more general approach to modeling of HVAC systems, and therefore the code discussed here is intended to be used as a tool that can model most practical HVAC systems of interest.

This paper focuses on the HVAC modeling code instead of the optimization algorithm. To be useful, the modeling code requires reasonable temperature and humidity predictions while still being computationally inexpensive. The code also needs to be adaptable to most HVAC systems of interest. Therefore, a lumped parameter code is proposed as a good balance between accuracy and computational efficiency. This code, called Lumped-HVAC (L-HVAC), provides reasonable predictions of transient and steady-state moist air properties in an HVAC system with known equipment and loads as will be demonstrated later in this report.

2. Code Algorithm

L-HVAC divides the moist air in the entire HVAC system into lumps of moist air mass. These lumps are defined as a fixed control volume within the

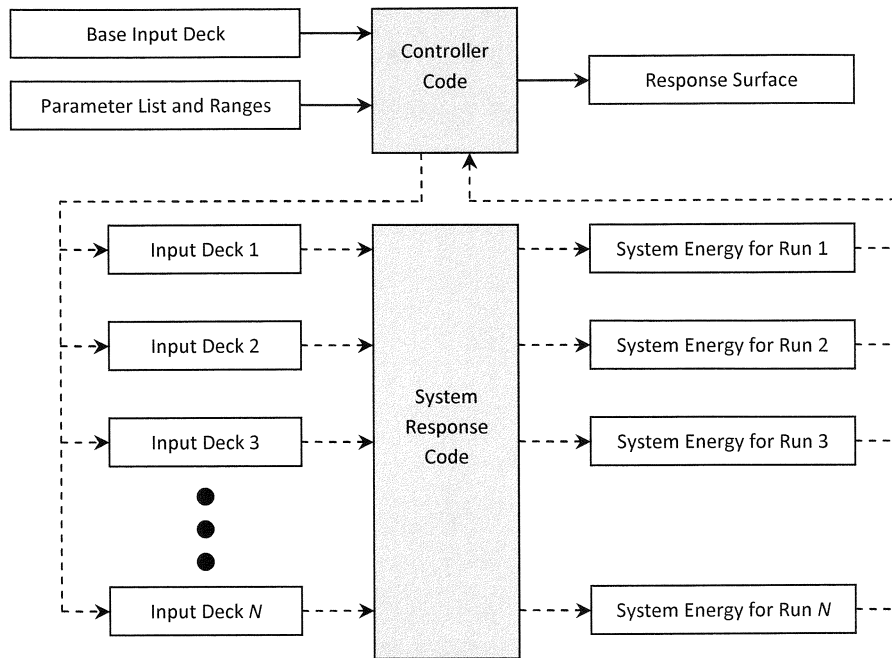


Figure 1: General algorithm for response surface generation.

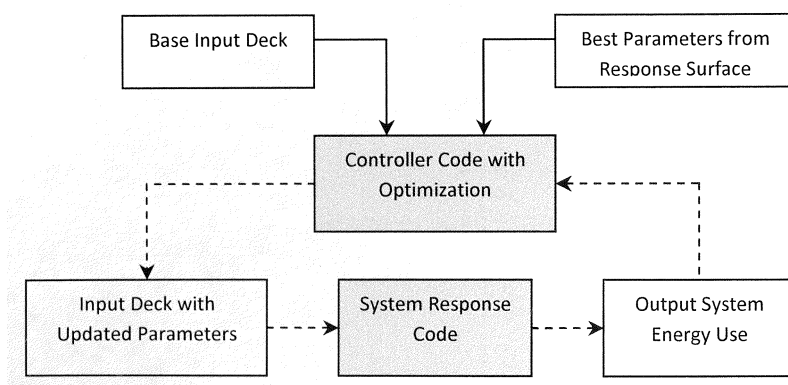


Figure 2: General algorithm for system optimization.

system, and at any given time the moist air in the control volume has uniform thermodynamic and psychrometric properties. Moist air flows between these lumps using defined paths that represent a tube of known cross-sectional size, length, and minor loss factor.

The approach to investigating a fluid system in this manner is not unique to L-HVAC: the code SINDA/FLUINT [14] applies the same formulation to a variety of fluid systems, and it is especially useful for systems where heat loss from the fluid to the surrounding environment is vital. The difference between L-HVAC and SINDA/FLUINT lies in L-HVAC's coupled water balance, psychrometric, and energy exchange calculations. SINDA/FLUINT contains external subroutine input capability, so it is possible that the commercial code could be adapted to allow for the same calculations presented here. In this study, SINDA/FLUINT is used in this study for validation of simple systems.

It should also be noted that the EnergyPlus [15] software package is widely used to model the thermal response of HVAC systems (e.g., [5]). EnergyPlus applies an explicit algorithm with non-coupled thermal and humidity balances, and it assumes incompressible flow. The explicit algorithm uses a predictor-corrector approach to allow for large (typically 0.1 to 0.25 hr) time steps. The size of the variable time step is based on the limitation of the maximum temperature rise in any zone in the simulation, which ignores the physical time step limitation of air available for infiltration between adjacent zones. L-HVAC, on the other hand, couples the thermal transport, humidity, and density variations in flow in an implicit fashion, and its variable time step sizes are based on this infiltration limit. The coupling of humidity variation with thermal transport allows for direct incorporation of latent heat loads into the optimization process, therefore providing an advantage for L-HVAC over EnergyPlus for applications featuring high latent heat. The effects of coupling will be demonstrated later in this report.

The L-HVAC algorithm comprises a set of layered nonlinear implicit solutions. All equations provided here are in SI units, but the code also allows for English units. Psychrometric calculations follow those provided in the ASHRAE Handbook of Fundamentals [16]. The code may be run in transient or steady-state mode, and a transient run may be continued from a previous state. The time step used is variable and defined as the minimum time for any lump in the simulation to transport all of its moist air to an adjacent downstream lump. Figure 3 graphically describes the following general algorithm:

- Solve the moist air flowrates and pressure drops through the duct system using a flow resistance calculation. These flow resistance calculations include calculations of pressure drop, and temperature and humidity adjustments to the moist air flow due to the presence of the coil.
- Solve the water mass balance in the system to obtain the humidity ratio distribution.
- Solve the energy balance in the system to obtain the moist air temperature distribution.
- Check for convergence; if not converged, then return to the flow resistance calculation with updated moist air density values.

Each of these points are now described.

2.1. Flow Resistance Calculations

If the density of the moist air is approximated to be constant, then the system may be set up according to a flow resistance network calculation. This approach is an extension of that discussed in numerous undergraduate fluid mechanics texts (e.g. [17, 18]), and it allows for simplified analysis of a complex fluid network. In general, the pressure drop in a single duct branch (Δp) is given by

$$\Delta p = Q^2 R_{flow} - \Delta p_{gain} + \Delta p_{loss} \quad (1)$$

where Q is volumetric flow rate, Δp_{gain} is the pressure rise due to a fan, Δp_{loss} is a pressure drop due to the presence of a coil, and R_{flow} is the flow resistance defined as

$$R_{flow} = \frac{\rho}{2} \left[\frac{1}{A_2^2} - \frac{1}{A_1^2} + \frac{\left(f \frac{L}{D_h} + \sum K_i \right)}{A^2} \right] \quad (2)$$

where ρ is mass density, A is area, D_h is hydraulic diameter, f is the Darcy friction factor, L is duct length, and K_i is a minor loss. In this equation, A_1 and A_2 , refer to the area at the entrance and exit of the duct, respectively, and A is the average area of the duct. The Appendix provides details on the derivation of this equation. Note that the SI units for R_{flow} are $[\text{kg}/\text{m}^7]$,

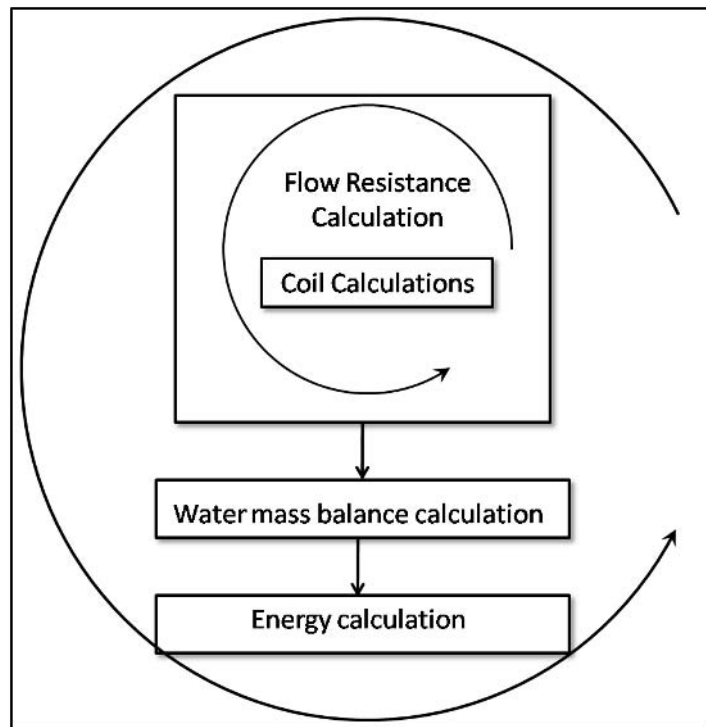


Figure 3: L-HVAC code algorithm.

which multiplied with volumetric flow rate [m³/s] squared yields a pressure drop in [Pa].

Coil calculations account for the Δp_{loss} term in Eq. 1. These calculations stem from reports by the Air-Conditioning and Refrigeration Institute (ARI) [19], and the equations account for the effects of partial or full condensation on the tubes, water loss due to condensation, pressure loss on both the air and refrigerant sides, and temperature rise in the refrigerant. Details of these calculations are too numerous to be included in this article. The Δp_{gain} term stems from the application of a fan.

The flow resistance calculation set includes pressure drop calculations along each branch following Eq. 1 and mass flow balance calculations at each lump:

$$\sum \rho_{in} Q_{in} = \sum \rho_{out} Q_{out} \quad (3)$$

where the subscripts *in* and *out* refer to the moist air streams into and out of the lump, respectively. A general formulation for this setup is written as the solution for a system of nonlinear equations:

$$d_{11}p_1 + d_{12}p_2 + \dots + d_{1M}p_M - R_{11}Q_1^2 - R_{12}Q_2^2 - \dots - R_{1N}Q_N^2 = \Delta p_{loss} - \Delta p_{gain} \quad (4)$$

$$D_{11}\rho_1^2Q_1^2 + D_{12}\rho_2^2Q_2^2 + \dots + D_{1N}\rho_N^2Q_N^2 = 2 \sum_{i=1}^{N_{in}} \sum_{j=i+1}^{N_{in}} \rho_i Q_i \rho_j Q_j - 2 \sum_{i=1}^{N_{out}} \sum_{j=i+1}^{N_{out}} \rho_i Q_i \rho_j Q_j \quad (5)$$

where the solution consists of a simultaneous solve of N instances of Eq. 4 for pressure drop along a path and M instances of Eq. 5 for mass flow balance at a lump. The solution vector contains all M unknown pressures (p_1, p_2, \dots, p_M) and N unknown flow rates squared ($Q_1^2, Q_2^2, \dots, Q_N^2$). The coefficients **d** and **D** in Eqs. 4 and 5 are either zero or one depending on the branch under consideration, and the coefficients **R** are either zero or the branch flow resistance R_{flow} depending on the branch under consideration. The terms on the right-hand side of Eq. 5 account for the nonlinearity of solving for flow rate squared when considering Eq. 3. Note that this adds a nonlinearity into the matrix solve, so a nonlinear solution with a relaxation factor is implemented to allow for convergence. This convergence is achieved when

the norm ϵ_{flow} falls below a user-defined value. The norm is defined as

$$\epsilon_{flow} = \sum_{i=1}^M \left| \frac{(p_i)_k - (p_i)_{k-1}}{(p_i)_{k-1}} \right| + \sum_{i=1}^N \left| \frac{(Q_i)_k - (Q_i)_{k-1}}{(Q_i)_{k-1}} \right| \quad (6)$$

where k is the iteration number.

2.2. Water Mass Balance Calculations

The flow resistance solution provides details regarding moist air flow rates in each duct in the system. Any changes in air humidity are accounted for in the water mass balance. In general, the increase in the amount of water m_w in a lump is defined by

$$\frac{\partial m_w}{\partial t} = \sum_{i=1}^{N_{in}} \dot{m}_{w,i} - \sum_{i=1}^{N_{out}} \dot{m}_{w,i} + \dot{m}_{inj} \quad (7)$$

where t is time, \dot{m}_w is the water mass flow rate, \dot{m}_{inj} is additional water injected into the lump, and N_{in} and N_{out} are the number of moist air streams into and out of the lump, respectively. Equation 7 may be expressed in terms of humidity ratio ω , the mass of dry air in the lump m_a , and the mass flow rate of dry air \dot{m}_a as

$$\frac{\partial (m_a \omega)}{\partial t} = \sum_{i=1}^{N_{in}} \dot{m}_{a,i} \omega_i - \sum_{i=1}^{N_{out}} \dot{m}_{a,i} \omega_i + \dot{m}_{inj} \quad (8)$$

This equation, expressed in terms of psychrometric density ρ (kg of dry air per m³ of mixture), is

$$\frac{\partial (\rho V \omega)}{\partial t} = \sum_{i=1}^{N_{in}} \rho_i Q_i \omega_i - \sum_{i=1}^{N_{out}} \rho_i Q_i \omega_i + \dot{m}_{inj} \quad (9)$$

where V is the lump volume. Since the lump volume is constant, Eq. 9 can be restated as

$$V \frac{\partial \xi}{\partial t} + \xi \left(\sum_{i=1}^{N_{out}} Q_i \right) - \left(\sum_{i=1}^{N_{in}} \xi_i Q_i \right) = \dot{m}_{inj} \quad (10)$$

where $\xi = \rho\omega$. For steady-state simulations or lumps with zero volume, this equation is written as

$$\xi \left(\sum_{i=1}^{N_{out}} Q_i \right) - \left(\sum_{i=1}^{N_{in}} \xi_i Q_i \right) = \dot{m}_{inj} \quad (11)$$

The implicit form of the transient and steady-state equations is thus

$$(\xi)_{p+1} \left(1 + \frac{\Delta t}{V} \sum_{i=1}^{N_{out}} Q_i \right)_{p+1} - \left(\frac{\Delta t}{V} \sum_{i=1}^{N_{in}} \xi_i Q_i \right)_{p+1} = (\xi)_p + \left(\frac{\Delta t}{V} \right) (\dot{m}_{inj})_{p+1} \quad (12)$$

$$(\xi)_{p+1} \left(\sum_{i=1}^{N_{out}} Q_i \right)_{p+1} - \left(\sum_{i=1}^{N_{in}} \xi_i Q_i \right)_{p+1} = (\dot{m}_{inj})_{p+1} \quad (13)$$

for time step p with size Δt . A system of N equations is solved simultaneously to obtain all N unknown values of $(\xi)_{p+1}$. Note that values of $(\xi)_p$ are updated at each iteration to account for density changes in the flow resistance calculation.

2.3. Energy Balance Calculations

The previous calculations provide values of moist air flow rates and water content in the system, which allows for determination of moist air properties in each lump based on psychrometrics and lump heating loads. A general energy balance in a lump follows

$$\frac{\partial E}{\partial t} = \sum_{i=1}^{N_{in}} \dot{E}_i - \sum_{i=1}^{N_{out}} \dot{E}_i + \dot{q} \quad (14)$$

where E is the energy in a lump, \dot{E} is the energy flow into or out of a lump due to moist air flow, and \dot{q} is the energy generated within a lump. The energy inside a lump may be expressed in terms of thermal and kinetic components:

$$E = m_a (C_{va} + \omega C_{vw}) T + m_a (1 + \omega) \frac{1}{2} \hat{V}^2 \quad (15)$$

where T is temperature, C_{va} and C_{vw} are the air and water specific heats at constant volume, respectively, and \hat{V} is moist air speed. Defining $\tilde{C}_v = C_{va} + \omega C_{vw}$ and $\eta = \rho \tilde{C}_v T$, Eq. 15 simplifies to

$$E = V \left[\eta + \rho (1 + \omega) \frac{1}{2} \hat{V}^2 \right] \quad (16)$$

The energy flow into the lump \dot{E} is

$$\dot{E} = \eta \tilde{Q} + \rho Q (1 + \omega) \frac{1}{2} \hat{V}^2 \quad (17)$$

where $\tilde{Q} = Q \frac{\tilde{C}_p}{\tilde{C}_v}$ and $\tilde{C}_p = C_{pa} + \omega C_{pw}$, where C_{pa} and C_{pw} are the dry air and water specific heat at constant pressure, respectively. Combining Eqs. 14, 16, and 17 for a fixed lump volume results in the expression

$$\begin{aligned} V \frac{\partial}{\partial t} \left[\eta + \rho (1 + \omega) \frac{1}{2} \hat{V}^2 \right] &= \sum_{i=1}^{N_{in}} \left[\eta_i \tilde{Q}_i + \rho_i Q_i (1 + \omega_i) \frac{1}{2} \hat{V}_i^2 \right] \\ &\quad - \sum_{i=1}^{N_{out}} \left[\eta_i \tilde{Q}_i + \rho_i Q_i (1 + \omega_i) \frac{1}{2} \hat{V}_i^2 \right] + \dot{q} \end{aligned} \quad (18)$$

The thermal terms are moved to the left side of the equation, and the kinetic energy terms are moved to the right side of the equation. Setting all η_i , ρ_i , and ω_i for the exiting streams equal to η , ρ , and ω , respectively, inside the lump yields

$$\begin{aligned} V \frac{\partial \eta}{\partial t} + \eta \sum_{i=1}^{N_{out}} \tilde{Q}_i - \sum_{i=1}^{N_{in}} \eta_i \tilde{Q}_i &= -V \frac{\partial}{\partial t} \left(\rho (1 + \omega) \frac{1}{2} \hat{V}^2 \right) \\ + \sum_{i=1}^{N_{in}} \left(\rho_i Q_i (1 + \omega_i) \frac{1}{2} \hat{V}_i^2 \right) - \rho (1 + \omega) \sum_{i=1}^{N_{out}} \left(Q_i \frac{1}{2} \hat{V}_i^2 \right) &+ \dot{q} \end{aligned} \quad (19)$$

For steady-state simulations or lumps with zero volume, Eq. 19 is simplified to

$$\eta \sum_{i=1}^{N_{out}} \tilde{Q}_i - \sum_{i=1}^{N_{in}} \eta_i \tilde{Q}_i = \sum_{i=1}^{N_{in}} \left(\rho_i Q_i (1 + \omega_i) \frac{1}{2} \hat{V}_i^2 \right) - \rho (1 + \omega) \sum_{i=1}^{N_{out}} \left(Q_i \frac{1}{2} \hat{V}_i^2 \right) + \dot{q} \quad (20)$$

The implicit formulation of Eqs. 19 and 20 at time step p is

$$\begin{aligned} \eta_{p+1} \left[1 + \frac{\Delta t}{V} \sum_{i=1}^{N_{out}} \tilde{Q}_i \right]_{p+1} - \left(\frac{\Delta t}{V} \sum_{i=1}^{N_{in}} \eta_i \tilde{Q}_i \right)_{p+1} &= (\eta)_p + \left[\rho (1 + \omega) \frac{1}{2} \hat{V}^2 \right]_p \\ - \left[\rho (1 + \omega) \frac{1}{2} \hat{V}^2 \right]_{p+1} + \frac{\Delta t}{V} \left(\sum_{i=1}^{N_{in}} \rho_i Q_i (1 + \omega_i) \frac{1}{2} \hat{V}_i^2 \right)_{p+1} \\ - \frac{\Delta t}{V} \left(\rho (1 + \omega) \sum_{i=1}^{N_{out}} \frac{1}{2} \hat{V}_i^2 \right)_{p+1} + \frac{\Delta t}{V} \dot{q}_{p+1} &(21) \end{aligned}$$

$$\eta_{p+1} \left[\sum_{i=1}^{N_{out}} \tilde{Q}_i \right]_{p+1} - \left[\sum_{i=1}^{N_{in}} \eta_i \tilde{Q}_i \right]_{p+1} = \left(\sum_{i=1}^{N_{in}} \rho_i Q_i (1 + \omega_i) \frac{1}{2} \hat{V}_i^2 \right)_{p+1} - \left(\rho (1 + \omega) \sum_{i=1}^{N_{out}} \frac{1}{2} \hat{V}_i^2 \right)_{p+1} + \dot{q}_{p+1} \quad (22)$$

These N equations are solved simultaneously for all N unknown values of η_{p+1} . As in the water mass balance calculations, the values of η_p are updated at each iteration to reflect changes in density and absolute humidity due to the flow resistance and water mass balance calculations, respectively.

2.4. Convergence and Energy Consumption Calculations

The Flow Resistance-Water Mass Balance-Energy Balance cycle continues until the solution converges below a user-defined tolerance. L-HVAC defines the norm ϵ at iteration k as

$$\epsilon = \sum_{i=1}^M \left| \frac{(\omega_i)_k - (\omega_i)_{k-1}}{(\omega_i^*)_{k-1}} \right| + \sum_{i=1}^M \left| \frac{(T_i)_k - (T_i)_{k-1}}{(T_i)_{k-1}} \right| \quad (23)$$

where $(\omega_i^*)_{k-1}$ equals $(\omega_i)_{k-1}$ if $(\omega_i)_{k-1} > 0$, or 1.0 if $(\omega_i)_{k-1} = 0$.

L-HVAC is tailored toward HVAC systems that contain a chiller that distributes chilled water to various heat exchangers in the HVAC system. Based on this assumption, energy is input to three locations in the system:

- Energy input to all pumps required to provide chilled water to the heat exchangers.
- Energy input to all fans required to provide airflow.
- Energy input to the chiller to cool the water.

In L-HVAC, the pumps and fans are defined based on one of 1) fixed pressure rise, 2) fixed flowrate, or 3) a user-defined fan curve. The pump/fan required power input is calculated as

$$\dot{E}_{pump/fan} = \frac{Q \Delta p}{\hat{\eta}_{pump/fan}} \quad (24)$$

where $\hat{\eta}_{pump/fan}$ is the pump/fan efficiency. The chiller power input is calculated as

$$\dot{E}_{chiller} = \frac{\dot{m}_w C_{pw} (\Delta T)_w}{COP_{chiller}} \quad (25)$$

where $COP_{chiller}$ is the chiller Coefficient of Performance, and $(\Delta T)_w$ is the change in temperature of the chilled water as it passes through the chiller. Steady-state simulations provide values of energy usage per time and transient simulations provide accumulated energy use.

2.5. Controls

The primary purpose of L-HVAC is to provide a means to predictively control HVAC conditions to allow for optimization per Figs. 1 and 2. Therefore, various types controls are available for implementation in the code. These controls include control dampers, variable fan/pump speeds, and variable chiller work input. The input mechanisms for these controls include thermostats and airflow regulators. Figure 4 shows the available pairing of input and output control mechanisms in L-HVAC. These controls follow a standard PID algorithm for an input voltage \tilde{V} based on deviation from setpoint $\Delta\iota$:

$$\tilde{V} = \tilde{V}_0 + \alpha_P \Delta\iota + \frac{\alpha_I}{t} \int_0^t \Delta\iota d\iota + \alpha_D \left(\frac{d(\Delta\iota)}{dt} \right) \quad (26)$$

where α_P , α_I , and α_D are three user-defined PID control coefficients. The use of PID algorithms is typical for HVAC modeling studies (e.g. [20]). Only α_P is used in steady-state simulations.

3. Validation Exercises

Several tests were performed to ensure proper operation of the code, including a test comparing L-HVAC simulations of dry air to commercial code calculations and an incompressible theoretical model, a test showing behavior of control mechanisms, and a test demonstrating experimental-computational validation. Note that additional tests were used to show that the discretization of the ductwork and the time step had no significant effect on the simulated results for the system described below.

3.1. Theoretical Validation - Dry Air and Fixed Humidity Ratio

L-HVAC was first validated by comparing its results to that by SINDA/FLUINT and a simplified theoretical model for the system shown in Fig. 5. The system features $0.117 \text{ m}^3/\text{s}$ of ventilation air at 21.1°C mixed with $0.395 \text{ m}^3/\text{s}$ of return air flowing into a room of volume 28.3 m^3 . The room contains a load

of 1460 W. If density changes in the air are not taken into account due to pressure variation in the system, the predicted temperature rise in the room is governed by the differential equation

$$\rho V C_{va} \frac{dT}{dt} + x \dot{m} C_{pa} (T - T_O) = \dot{q} \quad (27)$$

where T_O is the outside air temperature, and x is the volume fraction of external air into the room. The solution to this differential equation with $T(0) = T_O$ is

$$T(t) = T_O + \frac{\dot{q}}{x \dot{m} C_{pa}} \left[1 - \exp \left(-\frac{x \dot{m} C_{pa} t}{\rho C_{va} V} \right) \right] \quad (28)$$

Figure 6 shows that all three approaches provide similar results for this simple system. The differences in the curves may be attributed to different applied approximations in the code algorithms or theoretical model. In general, the predicted response by L-HVAC agrees better with the theoretical model than the SINDA/FLUINT results. The maximum difference in predicted values between L-HVAC and the theoretical model and the values between L-HVAC and SINDA/FLUINT is 0.3°C and 1.3°C , respectively, which occurs at 3.5 minutes. The average difference in values between L-HVAC and the theoretical model is 0.25°C , and the average difference in values between L-HVAC and SINDA/FLUINT is 0.48°C . Note that steady-state L-HVAC simulations obtain the same room temperature as transient simulations within 0.01°C for $t > 40$ min.

A modification of this test was used to ensure the uniformity of ω when no water is injected or removed from the system. The same system of Fig. 5 was initialized with a globally uniform relative humidity of 50%, no mass injection, and a 1460 W sensible heating load. The result shows that the system does not experience a change in ω greater than 0.002% of its initial value despite an increase in dry bulb temperature of 10.3°C , which is consistent with an overall mass balance of water in the system.

Another interesting result is that ω affects T . Analysis of Eq. 21 using Eq. 3 shows that even when kinetic energy terms are neglected, a lump initialized with a globally uniform dry bulb temperature, no heating loads, and water mass injection will still experience a change in dry bulb temperature due to different airstream heat capacity values influenced by unique values of ω in each airstream in the system. A modified version of the dry air simulation was produced to illustrate this fact. The sensible heat load in the

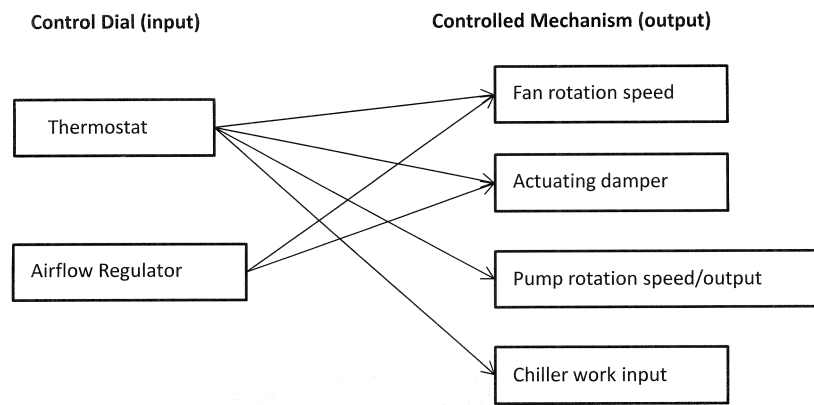


Figure 4: Input/Output control pairing options.

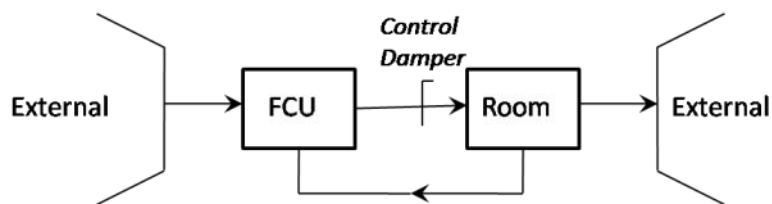


Figure 5: HVAC system model containing a single room and fan coil unit (FCU).

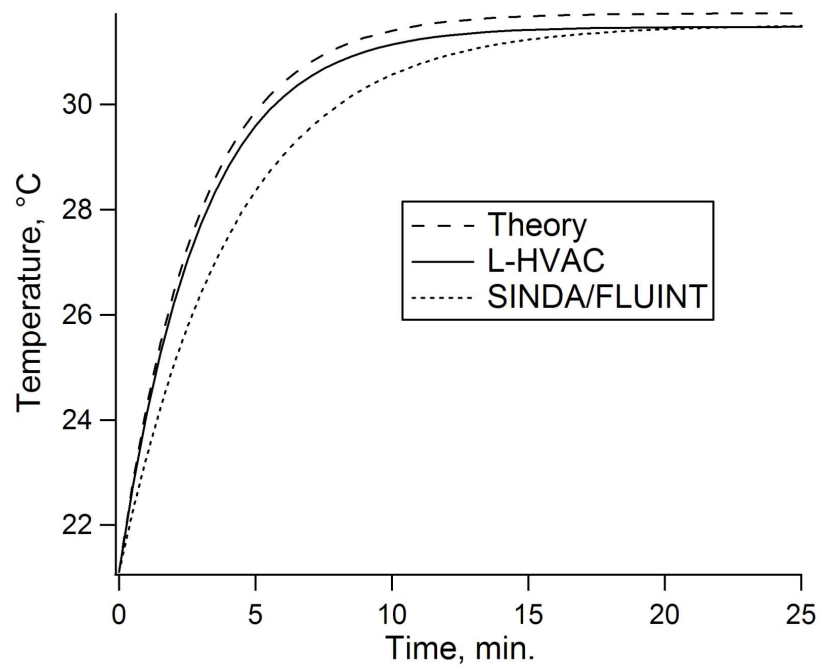


Figure 6: Theoretical validation via predictions of room temperature for a dry air system.

room was replaced with water injection of 0.756 kg/s. After 25 minutes, the room temperature dropped by 0.61°C, and the relative humidity increased to 59.4%.

3.2. Code Validation to Experiment and Analytical Model

A simple experiment and corresponding analytical model were used to validate the code. The lumped approximation is used for the analytical model. In the experiment, wet-bulb and dry-bulb measurements were taken during a classroom setting. The only air input to the classroom is through a wall-mounted fan to the ambient environment outside the building. Velocity measurements for the fan found an average input flow rate of 0.296 m³/s using a TycosTM vane anemometer, and an assumed ventilation rate of 0.5 air changes per hour per ASHRAE [21] provided an additional 0.0426 m³/s. The room volume was calculated from measurements to be 308 m³. The room exhaust was assumed to be the same as the input flow rate from the outside. An array of 16 ceiling fans were used to mix the air inside the room. Wet- and dry-bulb Temperature measurements were taken for 75 minutes using a Sierra-MiscoTM psychrometer, and psychrometric calculations were used to determine values of $\omega(t)$.

The analytical model applies a known mass flow rate of air from outside the building into the classroom. The total and latent loads for each of the 27 people in the room are 120 W and 44.0 W per person per ASHRAE [21]. The total amount of water injected into the room air is calculated from the latent heat to be 0.0291 kg/s using

$$\dot{m}_{inj} = \frac{N_p \dot{Q}_{lat}}{h_{fg}} \quad (29)$$

where N_p is the number of people in the room, \dot{m}_{inj} is the mass flowrate of water injected into the system, \dot{Q}_{lat} is latent heat, and h_{fg} is the latent energy of water per mass. A simple differential equation for the average system humidity are expressed as

$$\rho V \frac{d\omega}{dt} = \dot{m} (\omega_0 - \omega) + \dot{m}_{inj} \quad (30)$$

Figure 7 shows that a reasonable agreement in humidity ratio variation is achieved if the external ω is 0.0069, which corresponds to 75% relative humidity (RH) for 13°C air, which are reasonable external conditions for the time

of the experiment and considering the experimental error due to humidity gradients in the room and infiltration from other areas within the building. A dry bulb temperature validation is inadequate with this experiment as the effects from wall conduction, convection, and glazing effects provide too large of an experimental error.

3.3. Application of Controls for Energy Savings

Additional validation tests were performed to show the proper response by the simulated controls. In Fig. 5, a control damper is placed in the system at the inlet to the room. The room temperature setpoint is 26.7 °C for a cooling system containing a 3.517 kW chiller, a variable speed fan containing a single line fan curve connecting two points (700 Pa at 0 m³/s and 0 Pa at 0.7 m³/s), and a pump with 6.31×10^{-4} m³/s output. The efficiency of the fan and pump is 0.8, and the COP for the chiller is 3.0. The external conditions are 21.2°C and 50% RH. Figure 8 shows that the system response to reach the setpoint depends on the output device. Each output device uses Eq. 26 $\alpha_P \neq 0$ and $\alpha_I = \alpha_D = 0$.

Fig. 8 also shows that the steady-state temperature for a system without control is 23.6°C. A steady-state simulation of the system shows an energy use of 1.30 kW to attain this temperature. The energy savings per time for a room temperature setpoint of 26.7°C were calculated for system control via each mechanism using the formula

$$\dot{E}_{savings} = \dot{E}_{nc} - \dot{E}_c \quad (31)$$

where the subscripts *nc* and *c* refer to system power usage without controls and with controls, respectively. L-HVAC steady-state simulations can calculate energy savings for an infinite variation of conditions, arrangements and control strategies. Results clearly show the dominant energy consumption of the chiller and the coupled nature of various control strategies. For example, varying the fan airflow will also reduce the air conditioning load since less reduced airflow over the cooling coil will reduce the amount of heat transferred. A minimum quantity of airflow is required for proper circulation. The arrangement and cooling load variants will have a large effect on the energy savings for variable speed fans and some studies such as Teitel et al. [22] have reported savings as large as 25%.

Table 1: Effect of humidity on steady-state temperature prediction.

Latent Heat Fraction	Steady-State Temperature, °C
0%	31.5
20%	31.4
40%	31.3
60%	31.2
80%	31.2
100%	31.1

4. Effect of Coupling Humidity and Temperature

L-HVAC was designed to include the influence of humidity on temperature, thereby allowing for optimization of systems featuring high latent loads. The effect of humidity on temperature is demonstrated by adjusting the fraction of latent to total heat generation in the room. Table 1 shows that a variation of 0.4°C in resultant steady-state room air temperature when the ratio of latent heat load to total heat load is increased from 0% to 100%. Although the uncertainty in approximating the room air as uniform supercede this value, a fine discretization of a fluid system with high latent loads would benefit from incorporating the influence of humidity on the temperature calculation. This ability to incorporate the latent heat loads into the temperature calculation allows for the direct calculation of energy requirements for both temperature and humidity control by the HVAC system, and therefore optimization of HVAC energy use by systems with latent loads is feasible using L-HVAC.

5. Conclusion

The L-HVAC code presented here provides the basis for optimization of HVAC designs to meet a particular load distribution. The incorporation of control mechanisms and energy calculations within the code allow for a direct means to observe the system energy usage for various control settings. The code organization allows for the user to specify the accuracy of the temperature, humidity, and energy calculations based on the discretization level of the model. Future work on this project will require finer-resolution

models than that shown in Fig. 5, but the general approach to modeling the system will not change.

6. Acknowledgements

Research funding by the ASEE-ONR Summer Faculty Fellowship Program sponsored by Mark Spector, Ph. D.; conversations with Amip Shah of Hewlett-Packard; and experimental measurements by Eric Wroble are greatly appreciated.

- [1] D. o. E. Energy Information Administration, Table us-1. electricity consumption by end use in u. s. households, 2001.
- [2] C. L. B. P.E., In the data center, power and cooling costs more than the it equipment it supports, *Electronics Cooling*.
- [3] S. Greenberg, E. Mills, B. Tshudi, P. Rumsey, B. Myatt, Best practices for data centers: lessons learned from benchmarking 22 data centers, *ACEEE Summer Study on Energy Efficiency in Buildings* 3 (2006) 76–87.
- [4] J. F. Kreider, P. S. Curtiss, A. Rabl, *Heating and Cooling of Buildings; Design for Efficiency*, 2nd Edition, McGraw-Hill, 2002.
- [5] V. Congradac, F. Kulic, Hvac system optimization with co2 concentration control using genetic algorithms, *Energy and Buildings* 41 (5) (2009) 571–577.
- [6] S. Soyguder, H. Alli, Predicting of fan speed for energy saving in hvac system based on adaptive network based fuzzy inference system, *Expert Systems with Applications* 36 (4) (2009) 8631–8638.
- [7] L. Lu, W. J. Cai, L. H. Xie, S. J. Li, Y. C. Soh, Hvac system optimization - in-building section, *Energy and Buildings* 37 (1) (2005) 11–22.
- [8] A. Saltelli, K. Chan, E. M. Scott, *Sensitivity Analysis*, Wiley, 2000.
- [9] A. P. Wemhoff, A. K. Burnham, A. L. Nichols, Application of global kinetic models to hmx beta-delta transition and cookoff processes, *Journal of Physical Chemistry A* 111 (9) (2007) 1575–1584.

- [10] A. P. Wemhoff, W. M. Howard, A. K. Burnham, A. L. Nichols, An lx-10 kinetic model calibrated using simulations of multiple small-scale thermal safety tests, *Journal of Physical Chemistry A* 112 (38) (2008) 9005–9011.
- [11] K. F. Fong, V. I. Hanby, T. T. Chow, Hvac system optimization for energy management by evolutionary programming, *Energy and Buildings* 38 (3) (2006) 220–231.
- [12] K. F. Fong, V. I. Hanby, T. T. Chow, System optimization for hvac energy management using the robust evolutionary algorithm, *Applied Thermal Engineering* 29 (11-12) (2009) 2327–2334.
- [13] M. E. Snyder, T. A. Newell, Cooling cost minimization using building mass for thermal storage, in: 1990 Annual Meeting of the American Society of Heating, Refrigerating and Air-Conditioning Engineers, Technical and Symposium Papers, June 10, 1990 - June 13, 1990, ASHRAE Transactions, Publ by ASHRAE, St. Louis, MO, USA, 1990, pp. 830–838.
- [14] <http://www.crtech.com/sinda.html>.
- [15] <http://apps1.eere.energy.gov/buildings/energyplus/>.
- [16] ASHRAE Handbook of Fundamentals, American Society of Heating, Refrigerating, and Air Conditioning Engineers, 2001.
- [17] D. C. Wilcox, Basic Fluid Mechanics, 1st Edition, DCW Industries, 1997.
- [18] R. W. Fox, P. J. Pritchard, A. T. McDonald, Introduction to Fluid Mechanics, 7th Edition, Wiley, 2009.
- [19] 2001 Standard for Forced-Circulation Air-Cooling and Air-Heating Coils, Standard 410, Air-Conditioning and Refrigeration Institute, 2001.
- [20] Q. Bi, W.-J. Cai, Q.-G. Wang, C.-C. Hang, L. Eng-Lock, Y. Sun, K.-D. Liu, Y. Zhang, B. Zou, Advanced controller auto-tuning and its application in hvac systems, *Control Engineering Practice* 8 (6) (2000) 633–644.
- [21] ASHRAE Handbook of Fundamentals, American Society of Heating, Refrigerating, and Air Conditioning Engineers, 1989.

- [22] M. Teitel, A. Levi, Y. Zhao, M. Barak, E. Bar-Lev, D. Shmuel, Energy saving in agricultural buildings through fan motor control by variable frequency drives, *Energy and Buildings* 40 (6) (2008) 953–960.

7. Appendix: Derivation of Flow Resistance Relation

The standard relation for incompressible, viscous internal flow between two axial locations in a duct (defined here as locations 1 and 2) is [17, 18]

$$\left(\frac{p}{\rho g} + \hat{\alpha} \frac{\hat{V}^2}{2g} + z \right)_1 - \left(\frac{p}{\rho g} + \hat{\alpha} \frac{\hat{V}^2}{2g} + z \right)_2 = H_L - H_{gain} + H_{loss} \quad (32)$$

where $\hat{\alpha}$, H_L , g , and z are the kinetic coefficient, duct head loss, gravitational acceleration, and elevation, respectively; and H_{gain} and H_{loss} are the additional head gain and loss due to the presence of fans and coils, respectively. This equation may be rewritten as

$$\Delta p = (p_1 - p_2) = \rho g \left[\hat{\alpha}_2 \frac{\hat{V}_2^2}{2g} - \hat{\alpha}_1 \frac{\hat{V}_1^2}{2g} + (z_2 - z_1) + H_L \right] - \Delta p_{gain} - \Delta p_{loss} \quad (33)$$

where $\Delta p_{gain} = \rho g H_{gain}$ and $\Delta p_{loss} = \rho g H_{loss}$. If turbulent flow is assumed, then $\hat{\alpha}_1 = \hat{\alpha}_2 = 1$. Furthermore, potential energy changes may also be assumed to be negligible due the low density of air. These assumptions simplify Eq. 33 to

$$\Delta p = \frac{\rho}{2} \left[\hat{V}_2^2 - \hat{V}_1^2 + 2g \left(\frac{\hat{V}^2}{2g} \left(f \frac{L}{D_h} + \sum K_i \right) \right) \right] - \Delta p_{gain} - \Delta p_{loss} \quad (34)$$

where the head loss is expressed as

$$H_L = \frac{\hat{V}^2}{2g} \left(f \frac{L}{D_h} + \sum K_i \right) \quad (35)$$

Since $Q = \hat{V}A$, Eq. 34 may be expressed as

$$\Delta p = Q^2 \frac{\rho}{2} \left[\frac{1}{A_2^2} - \frac{1}{A_1^2} + \frac{1}{A^2} \left(f \frac{L}{D_h} + \sum K_i \right) \right] - \Delta p_{gain} - \Delta p_{loss} \quad (36)$$

or

$$\Delta p = Q^2 R_{flow} - \Delta p_{gain} - \Delta p_{loss} \quad (37)$$

where the flow resistance is defined as

$$R_{flow} = \frac{\rho}{2} \left[\frac{1}{A_2^2} - \frac{1}{A_1^2} + \frac{1}{A^2} \left(f \frac{L}{D_h} + \sum K_i \right) \right] \quad (38)$$

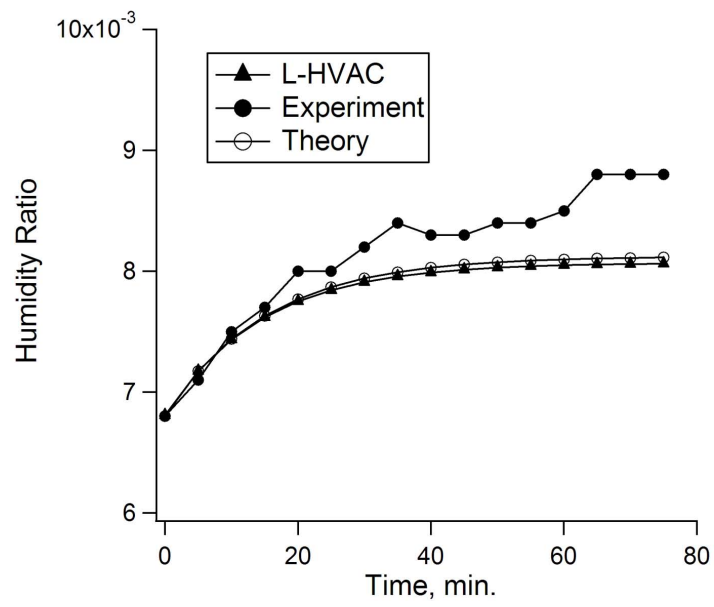


Figure 7: Comparison of L-HVAC prediction of $\omega(t)$ to predictions by Eq. 30 and experimental measurements.

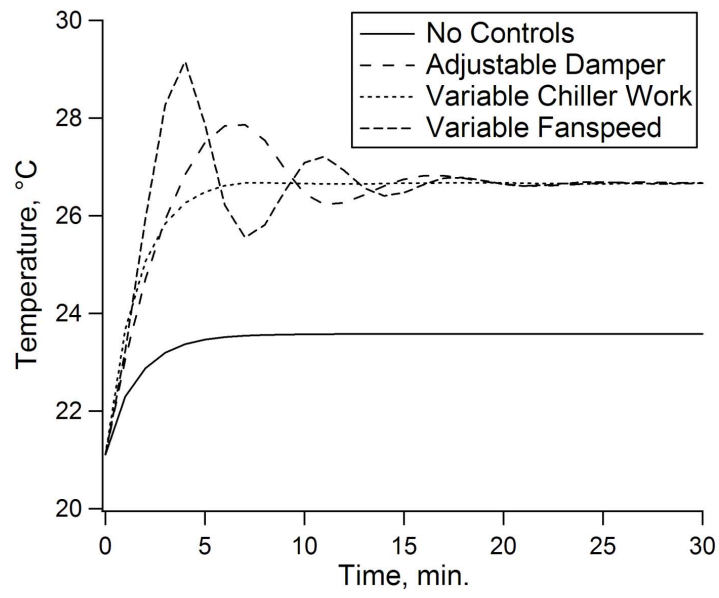


Figure 8: Implementation of various control devices into a simulated HVAC system. Controls contain a setpoint of 26.7°C . The adjustable damper, variable chiller work input, and variable fanspeed contain values of α_P of -1.0, 0.1, and 1.0, respectively.